Scientific Research Publishing

Advances in Remote Sensing, 2026, 15(2), 23-39
https://www.scirp.org/journal/ars
ISSN Online: 2169-2688
ISSN Print: 2169-267X

Seasonal Dynamics of Land Surface Temperature in Urban Louisiana: A Landsat 9-Based Analysis of New Orleans and Baton Rouge

Yaw A. Twumasi[1*], Olipa Simon[2], Edmund C. Merem[3], Zhu H. Ning[1], Harriet B. Yeboah[4], Priscilla M. Loh[1], Jeff D. Osei[1]

[1]Department of Urban Forestry, Environment and Natural Resources, Southern University and A&M College, Baton Rouge, LA, USA
[2]Institute of Resource Assessment, University of Dar es Salaam, Dar es Salaam, Tanzania
[3]Department of Urban and Regional Planning, Jackson State University, Jackson, MS, USA
[4]Department of Geography and Tourism Studies, Brock University, St. Catharines, Ontario, Canada
Email: *yaw.twumasi@sus.edu

How to cite this paper: Twumasi, Y.A., Simon, O., Merem, E.C., Ning, Z.H., Yeboah, H.B., Loh, P.M. and Osei, J.D. (2026) Seasonal Dynamics of Land Surface Temperature in Urban Louisiana: A Landsat 9-Based Analysis of New Orleans and Baton Rouge. *Advances in Remote Sensing*, **15**, 23-39.
https://doi.org/10.4236/ars.2026.152002

Received: October 9, 2025
Accepted: April 25, 2026
Published: April 28, 2026

Abstract

Urbanization and climate change have led to rising land surface temperatures (LST) in Louisiana's cities, particularly New Orleans and Baton Rouge, where impervious surfaces and reduced vegetation intensify the urban heat island effect. This study examines seasonal and spatial LST dynamics in these two urban areas to provide insights for targeted climate adaptation. Landsat 9 Operational Land Imager (OLI) thermal infrared data were analyzed, with LST derived from digital values converted to top-of-atmosphere spectral radiance, brightness temperature, and adjusted using land surface emissivity calculated from NDVI. The study fills research gap by comparing both cities using consistent methods to reveal shared and city-specific temperature pattern. Results revealed distinct seasonal variations in land surface temperature (LST), with Baton Rouge exhibiting a mean of 32.53˚C in the dry season and 19.26˚C in the wet season. In contrast, New Orleans recorded 30.90˚C and 18.85˚C, respectively. Spatial study indicated increased temperature fluctuation in New Orleans, with a greater proportion of land surpassing 35˚C during the dry season. These variations are attributed to fluctuations in surface moisture levels, vegetation density, and urban land use. The research illustrates the effectiveness of thermal infrared satellite data in evaluating urban thermal dynamics. It offers significant insights for climate monitoring, environmental planning, and the formulation of localized heat mitigation methods in humid Subtropi-

cal areas. Louisiana's urban planning bodies should adopt green infrastructure initiatives, such as expanding tree coverage, installing green roofs, and utilizing permeable materials to help curb rising land surface temperatures and lessen urban heat island impacts. In addition, using localized heat vulnerability maps can support more effective resource distribution and emergency planning with a focus on protecting neighborhoods most vulnerable to seasonal heat.

Keywords

Urban Heat Island, Subtropical Climate, Vegetation, Thermal, Land Cover, Remote Sensing

1. Introduction

Urban areas across the globe are experiencing rising land surface temperatures (LST) due to increasing urbanization and climate change. As cities expand and replace vegetation with impervious surfaces like roads and buildings, they absorb and retain more heat, intensifying the urban heat island (UHI) effect [1]. This effect leads to higher ambient temperatures in cities compared to surrounding rural areas, resulting in increased energy use, poorer air quality, and greater public health risks, especially during the summer months [2] [3].

Urban land surface temperature (LST) patterns have become an important area of study as cities around the world face growing environmental challenges related to climate change, rapid development, and uneven exposure to extreme heat. LST refers to the radiative skin temperature of the ground surface, which varies in response to factors, such as land cover, urban morphology, vegetation density, and proximity to water bodies [4]. In urban areas, the replacement of natural surfaces with impervious materials such as asphalt and concrete can cause significant increases in surface temperature, contributing to the formation of urban heat islands (UHIs) which happen to be zones where urban areas are significantly warmer than their rural surroundings [5] [6]. These patterns are not only spatially heterogeneous but also vary with the seasons, creating complex thermal environments that pose challenges for urban planning, public health, and climate adaptation.

Louisiana's unique geography and climate make it particularly vulnerable to seasonal thermal fluctuations. With a humid subtropical climate, abundant water bodies, and frequent extreme weather events, urban centers such as New Orleans and Baton Rouge face significant environmental challenges [7]. These cities are situated in low-lying areas adjacent to the Mississippi River and Lake Pontchartrain, where variations in land use and vegetation can drastically alter LST patterns [8]. Understanding the spatial and seasonal variation in LST is essential for climate adaptation and public health planning, especially as climate change increases the frequency and intensity of heat waves.

In the southern United States, particularly in Louisiana, these dynamics are further intensified by the region's humid subtropical climate. Characterized by long,

hot summers and mild winters, Louisiana cities are highly susceptible to prolonged heat exposure and associated health risks, especially for vulnerable populations in dense urban cores [2] [3]. Moreover, the state's flat topography, extensive water systems, and legacy of uneven urban development have led to a mosaic of thermal conditions across cities such as New Orleans and Baton Rouge. These two major urban centers, each shaped by unique historical, geographic, and environmental contexts both exhibit varying degrees of urban expansion, green infrastructure, and flood mitigation efforts, all of which play important roles in regulating LST at both micro and macro scales.

New Orleans, located below sea level and bounded by Lake Pontchartrain and the Mississippi River, presents a distinctive urban landscape where natural and built environments interact in complex ways. The city's mix of historical districts, canal networks, and levee systems influences its surface temperatures and the distribution of urban heat [9]. In contrast, Baton Rouge, situated on higher ground along the Mississippi River, has experienced more recent suburban growth and commercial expansion, leading to a different pattern of land use and thermal exposure. Both cities, however, face mounting pressure from climate-related stressors such as extreme heat, hurricanes, and heavy rainfall events issues that necessitate the need for a more granular understanding of LST trends at the urban scale.

Remote sensing technologies, particularly the use of satellite-derived thermal imagery, have enabled researchers to monitor LST across urban areas with increasing precision. The Landsat series, with its decades-long archive and 30-meter spatial resolution, has become a foundational tool for identifying seasonal and spatial variations in LST in cities worldwide, including those in the Gulf South [10]. These tools are especially valuable in Louisiana, where land-water interactions, vegetation dynamics, and development pressures vary sharply across neighborhoods and between cities.

By examining surface temperature patterns over time and space in urban Louisiana, particularly in New Orleans and Baton Rouge, researchers can better understand how local land cover, water proximity, and seasonal shifts affect urban microclimates. These insights are crucial for informing resilient infrastructure, urban forestry programs, and public health interventions in a region that is both ecologically rich and socioeconomically diverse. This study provides valuable insights into the seasonal behavior of land surface temperature in two major Louisiana cities and highlights the importance of urban vegetation, land cover, and moisture availability in moderating urban heat. The results not only illuminate existing thermal disparities but also offer a scientific basis for designing more climate-resilient urban landscapes in the face of rising temperatures and increasingly frequent extreme heat events. The paper therefore analyzes seasonal variations in land surface temperature (LST) in New Orleans and Baton Rouge by utilizing the reliable and high-resolution data provided by Landsat 9. Through this approach, it explores how differences in urban design and environmental factors influence surface temperature patterns across time. The findings offer valuable guidance for

developing targeted, city-level strategies to improve resilience against the growing threats of climate change. Even though numerous studies have explored the dynamics of land surface temperature (LST) and urban heat islands (UHI), the majority of this research tends to focus on single-city analyses, often overlooking how urban form and environmental context shape thermal patterns across cities within the same region. In the case of Louisiana, most prior studies either concentrate on New Orleans or Baton Rouge in isolation, rarely addressing how differences in urban morphology, vegetation cover, and proximity to water bodies affect seasonal LST patterns across cities.

Hence, this study addresses that gap by conducting a comparative, seasonally-disaggregated analysis of LST in both New Orleans and Baton Rouge using consistent remote sensing methods. By doing so, it highlights both shared and city-specific drivers of thermal variability, offering a broader and more nuanced perspective on urban thermal dynamics in the Gulf South. This comparative approach contributes new insights into how urban form and environmental context interact to influence surface temperatures which is crucial for developing more geographically tailored and equitable climate adaptation strategies.

2. Methodology

2.1. Study Area

Baton Rouge, commonly referred to as the Capital City is home to around 22% of Louisiana's total population. According to the U.S. Census Bureau, East Baton Rouge Parish has an estimated population of approximately 456,781 people [7]. It is renowned for its antique architecture, vast communities, and ethnic diversity. The parish is located in southeast Louisiana, along the eastern bank of the Mississippi River, and is estimated to be 1229 square kilometers in size. Due to its humid subtropical climate, Baton Rouge experiences hot, muggy summers and mild winters. The city has a bimodal rainfall pattern, meaning that spring and summer usually have the most precipitation. Numerous rivers and bayous, such as the Comite River and Bayou Fountain, drain the area, and they are essential to the hydrology and dynamics of urban flooding.

Situated in the southeast corner of Louisiana, Orleans Parish—New Orleans—is bordered to the north by Lake Pontchartrain and to the south by the Mississippi River. The most famous and historic city in Louisiana is New Orleans, which has a population of roughly 376,971, according to the 2020 census [8]. The parish requires an advanced system of levees and pumping systems because it is below sea level in several areas and covers an area of about 906 square kilometers. New Orleans is known for its colonial architecture, rich cultural legacy, and energetic urban life. It has long been referred to as "The Crescent City" because of its curved shape along the river. Due to its humid subtropical climate, the region experiences long, hot summers and brief, moderate winters. Significant summertime precipitation, frequently coupled with hurricanes and tropical storms, characterizes the rainfall pattern.

Both cities, New Orleans and Baton Rouge as seen in (Figure 1) are important Louisiana cities that serve as important government centers, business, education, and culture. Their geographical positions, ecological traits, and histories of urbanization offer a wealth of background information for environmental and spatial research land cover and surface moisture availability.

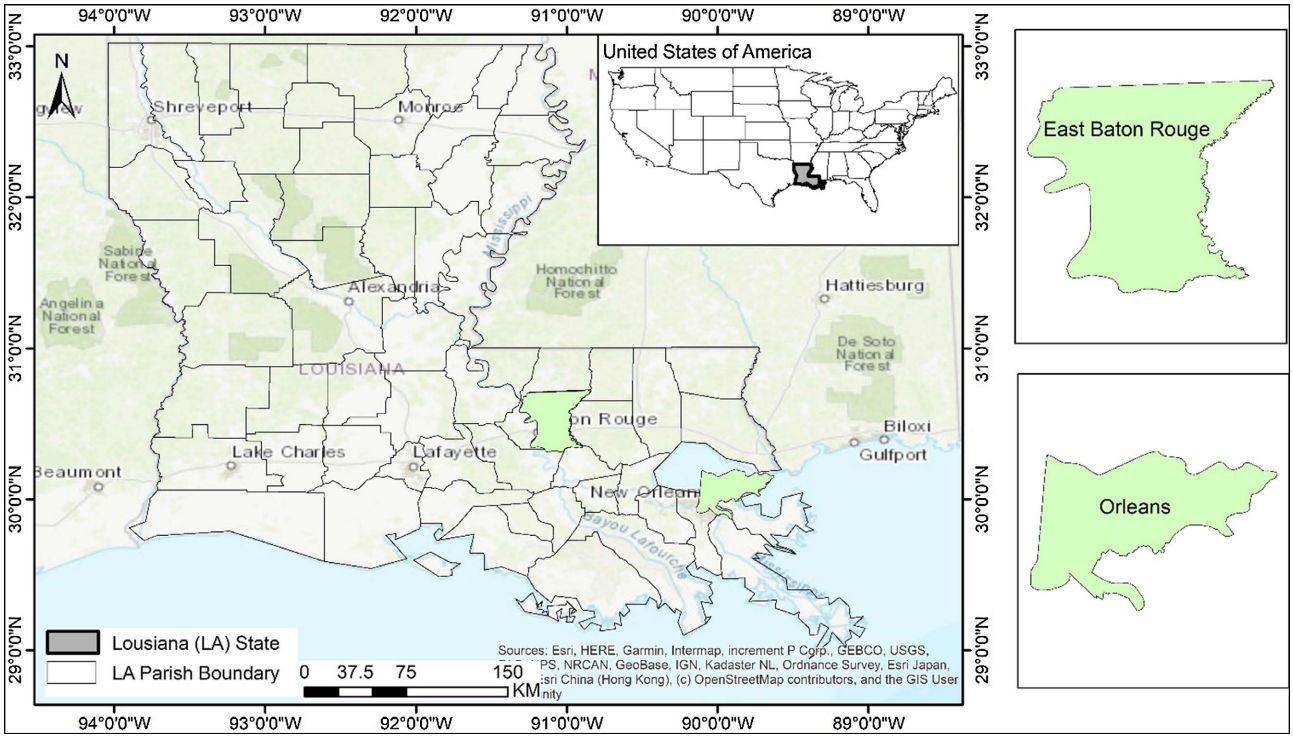

Figure 1. Study area.

2.2. Data Collection

This investigation employed Landsat 9 Level 2 Surface Reflectance and Surface Temperature products (Collection: LANDSAT/LC09/C02/T1_L2). These datasets offer atmospherically corrected surface reflectance bands, thermal infrared bands, and quality evaluation data, rendering them appropriate for land surface temperature (LST) research. Although the Level 2 products include a pre-calculated LST band, the LST was recalculated from the thermal infrared band to enable site-specific corrections and maintain consistency with previous studies.

The Landsat 9 images were obtained via the Operational Land Imager (OLI) and Thermal Infrared Sensor (TIRS) sensors. The data about New Orleans and Baton Rouge parishes in Louisiana were obtained from the United States Geological Survey (USGS) Earth Explorer platform through complimentary online services (https://earthexplorer.usgs.gov/). The images were chosen to depict the dry and wet seasons 2024, featuring less than 10% cloud cover to guarantee clarity and precision in thermal retrieval.

In southern Louisiana, the dry season typically spans from May to September, while the wet season occurs between November and April [11]. The selection of

seasonal images was predicated on these climatological behaviors. Figure 2 and Figure 3 illustrate the spatial extents of the selected Landsat 9 scenes, while Table 1 summarizes the utilized images. Supplementary data, including parish boundaries, were acquired from administrative shapefiles to define the area of interest (AOI).

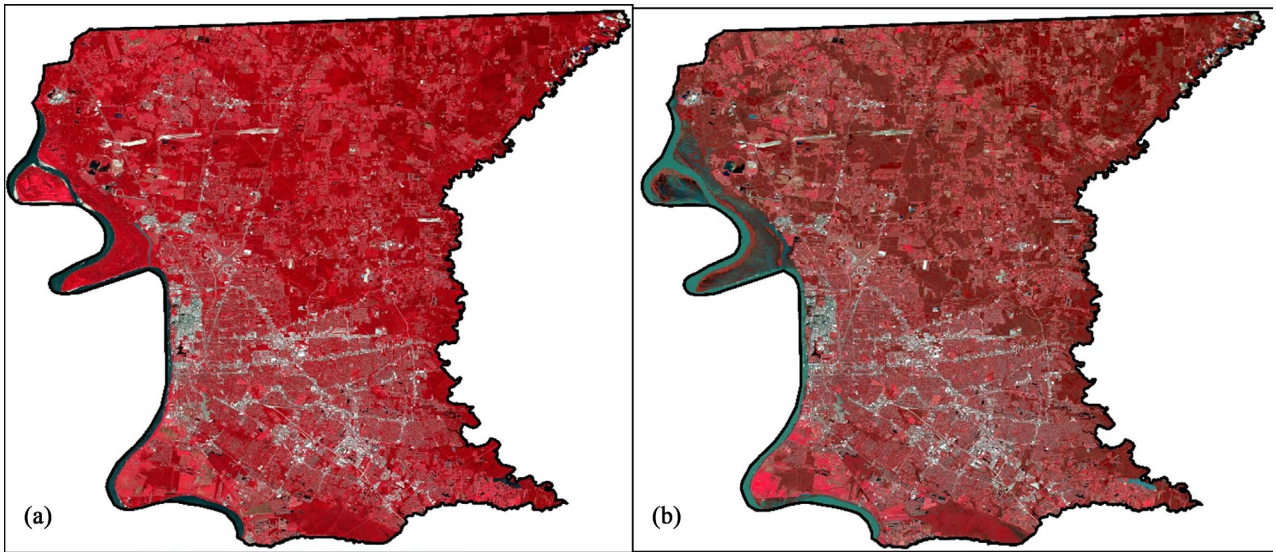

Figure 2. Landsat 9 Scene Maps of Baton Rouge Parish. Spatial Coverage of Selected Landsat 9 Scenes for Baton Rouge Parish Used in the LST Study shown in false color composite from (a) dry season and (b) Rainy season.

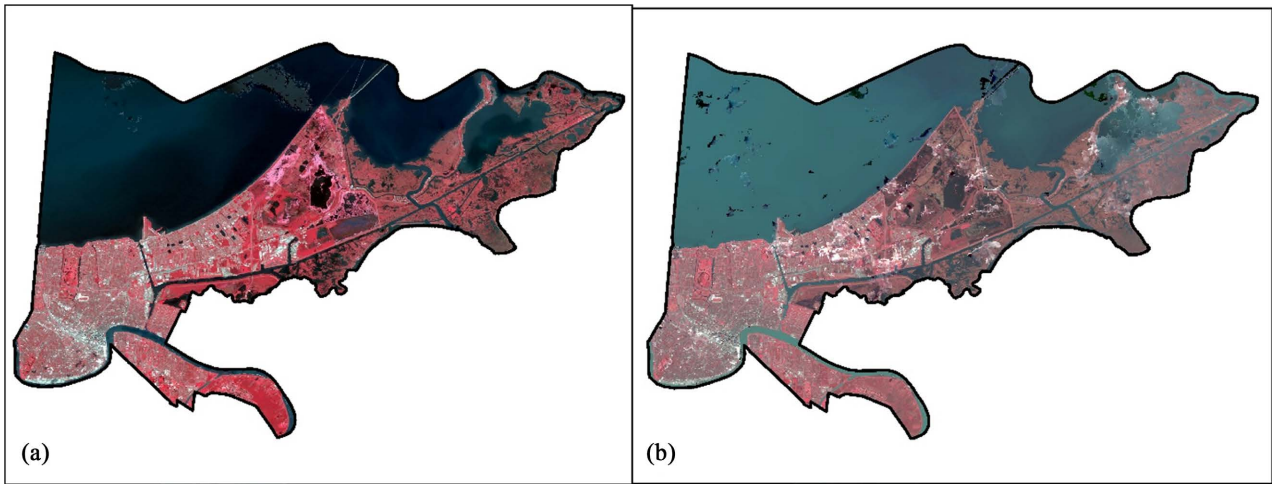

Figure 3. Landsat 9 Scene Maps of New Orleans Parish. Spatial Coverage of Selected Landsat 9 Scenes for New Orleans Parish Used in the LST Study shown in false color composite from (a) dry season and (b) Rainy season.

Table 1. Landsat 9 imagery used for LST analysis in Baton Rouge and New Orleans, Louisiana during the dry and rainy seasons (2024).

Reference year	Resolution	WRS: P/R	Date of Acquisition	Season	Study area
2024	30 m	23/039	2024/09/03	Dry	Baton Rouge
2025	30 m	23/039	2025/03/18	Rainy	Baton Rouge
2024	30 m	22/039	2024/09/03	Dry	New Orleans
2025	30 m	22/039	2025/03/20	Rainy	New Orleans

All image processing, analysis, and visualization were performed with Google Earth Engine (GEE) for cloud-based data management and ArcGIS 10.8 for mapping and layout design.

2.3. Image Preprocessing

Image preprocessing was implemented using Google Earth Engine open-source code function for cloud, shadow, and snow masking for Landsat 5 images [12]. The preprocessing includes stacking individual bands, cloud masking, radiometric correction, and clipping the stack to the study areas. Cloud masking and gap-filling were completed using the Quality Assessment bands. To ensure consistency in spatial analysis and temporal change detection, all imagery was reprojected to the Universal Transverse Mercator (UTM) coordinate system, Zone 15 North, corresponding to the Louisiana region. The datum and spheroid were based on WGS84, which aligns with the U.S. national topographic mapping standards.

Finally, the Landsat images were subsequently imported into ArcGIS 10.8 for further processing. During the preprocessing stage, both visual inspection and digital enhancement techniques were applied to improve image quality and prepare the data for analysis. Thermal Infrared bands—specifically Bands 10 and 11—were selected for Land Surface Temperature (LST) analysis. A shapefile covering New Orleans and Baton Rouge was used to clip the full scenes and extract the area of interest for focused analysis.

2.4. Image Analysis

The algorithm was created in ArcGIS 10.8. This study used Landsat 9 Thermal Infrared bands (Band 10 and Band 11) to estimate brightness temperature, and bands 4 and 5 were used for calculating the NDVI. The LST retrieval formulas were taken from the USGS web page (https://www.usgs.gov/core-science-systems/nli/landsat/using-usgs-landsat-level-1-data-product) for retrieving the Top of atmospheric (TOA) spectral radiance. The LST was retrieved following the steps of **Figure 4**.

2.5. Land Surface Temperature (LST) Estimation

Land Surface Temperature (LST) was derived using a structured set of mathematical algorithms based on thermal infrared (TIR) band data and variations in surface emissivity, following the approach of [14]. The procedure consisted of three main steps: converting digital numbers (DN) to spectral radiance, transformation into brightness temperature, and correction using land surface emissivity.

2.5.1. Conversion of Digital Numbers to Atmospheric Spectral Radiance (TOA)

Raw satellite digital values were initially converted into at-sensor spectral radiance to create a standardized radiometric scale. The radiometric calibration outlined by [15] guarantees uniformity among Landsat sensors. For Level 1 products, spectral radiance (L_λ) was computed using Equation (1) below:

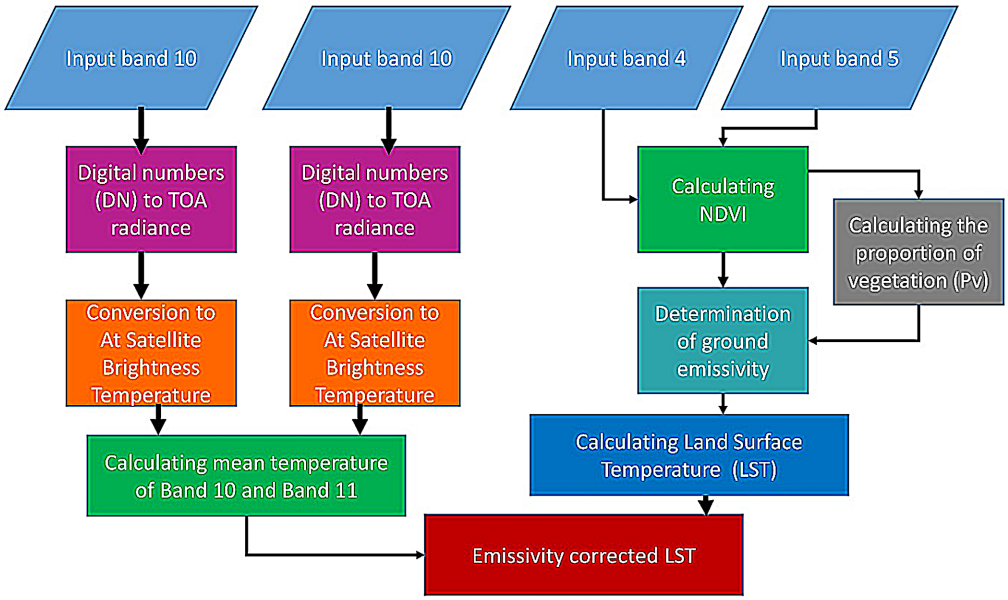

Figure 4. Flowchart for LST retrieval (Adapted from [13]).

$$L_\lambda = \frac{L_{\max\lambda} - L_{\min\lambda}}{Q_{\text{Calmax}} - Q_{\text{Calmin}}} * \left(Q_{\text{Cal}} - Q_{\text{Calmin}}\right) + L_{\min\lambda} \quad (1)$$

where:

L_λ: spectral radiance at the sensor's aperture ($W \cdot m^{-2} \cdot sr^{-1} \cdot \mu m^{-1}$);

Q_{Cal}: Quantified calibrated pixel value (DN);

Q_{calmin} Q_{calmax}: Minimum and maximum quantized DN values;

$L_{\min\lambda}$ $L_{\max\lambda}$: is Spectral radiance corresponding to Q_{calmin} and Q_{calmax}.

2.5.2. Conversion of TOA to Brightness Temperature

The next step involved converting spectral radiance to at-satellite brightness temperature (T_b) in degrees Celsius, using the inverse Planck function in Equation (2) as shown below [16].

$$T_b = \frac{K_2}{\ln\left(\frac{K_1}{L_\lambda} + 1\right)} - 273.15 \quad (2)$$

where:

T_b = Top of atmosphere brightness temperature (K);

L_λ = TOA spectral radiance (Watts/(m^{2*}srad*μm));

K_1 = Band-specific thermal conversion constant from the metadata;

K1_CONSTANT_BAND_x, where x is the thermal band number;

K_2 = Band-specific thermal conversion constant from the metadata;

K2_CONSTANT_BAND_x, where x is the thermal band number.

2.5.3. Estimation of NDVI

The Normalized Difference Vegetation Index (*NDVI*), obtained from satellite imagery, is a crucial indication of vegetation health and is frequently employed to

evaluate drought conditions. *NDVI* is calculated using Equation (3) by examining the differential reflectance of red and near-infrared (*NIR*) light, generally utilizing Band 4 (red) and Band 5 (*NIR*) from Landsat data. This measure offers insight into the density and intensity of green vegetation on the land surface.

Estimating *NDVI* is essential, as it directly indicates the quantity of living vegetation, a critical input for subsequent computations. *NDVI* is utilized to calculate the proportion of vegetation (P_v), which is crucial for determining land surface emissivity (ε), a parameter necessary for precise land surface temperature (LST) assessment [13]

$$NDVI = \frac{NIR(\text{band } 5) - R(\text{band } 4)}{NIR(\text{band } 5) + R(\text{band } 4)} \tag{3}$$

NIR represents the near-infrared band (Band 5), and *R* represents the red band (Band 4).

2.5.4. Calculating the Proportion of Vegetation

The Vegetation Fraction is the fraction of the ground area occupied by vegetation in vertical projection. It directly influences surface water and energy budgets through its effects on plant transpiration, surface albedo, emissivity, and roughness [17]. The vegetation proportion, P_v, is closely associated with *NDVI* values for vegetation and soil. In this study, P_v was assessed using the conventional *NDVI* methodology [18] in Equation (4).

$$P_v = \left(\frac{NDVI - NDVI_s}{NDVI_v - NDVI_s} \right)^2 \tag{4}$$

NDVI is the normalized difference vegetation index calculated from Landsat images' red and near-infrared bands where $NDVI_v$ and $NDVI_s$ are Maximum and Minimum *NDVI*, respectively, representing *NDVI* of Vegetation and *NDVI* of soil, respectively

2.5.5. Determining Land Surface Emissivity

Land Surface Emissivity (LSE). The average emissivity of a surface element of the Earth is derived from measured radiance and land surface temperature. The land surface emissivity (LSE (ε)) is essential for estimating land surface temperature (LST), as it serves as a proportionality factor that scales blackbody radiance according to Planck's Equation (5) to predict emitted radiance. It also reflects the efficiency of thermal energy transfer from the surface to the atmosphere, while the ground emissivity is determined conditionally [19].

$$\varepsilon_\lambda = \varepsilon_{v\lambda} p_v + \varepsilon_{s\lambda} (1 - p_v) + c_\lambda \tag{5}$$

In this context, ε_v and ε_s denote the emissivities of vegetation and soil, respectively. In contrast, C signifies surface roughness ($C = 0$ for homogeneous and flat surfaces), assigned a constant value of 0.005 [20]. The condition can be expressed using the subsequent formula in Equation (6) and the specified emissivity constant values [13].

$$\varepsilon_{\lambda} = \begin{cases} \varepsilon_{s\lambda}, & NDVI < NDVI_s, \\ \varepsilon_{v\lambda} P_v + \varepsilon_{s\lambda}\left(1 - P_v\right) + C, & NDVI_s \le NDVI \le NDVI_v, \\ \varepsilon_{s\lambda} + c, & NDVI > NDVI_v. \end{cases} \quad (6)$$

If the *NDVI* is below 0, it is categorized as water, with an emissivity value of 0.991 applied. *NDVI* values ranging from 0 to 0.2 indicate soil coverage, with an assigned emissivity value of 0.996. Values ranging from 0.2 to 0.5 are deemed a mixture of soil and vegetation cover and are utilized to obtain emissivity [1]. In the final scenario, an *NDVI* value exceeding 0.5 indicates vegetation coverage, with a corresponding value of 0.973 applied. For this study, the mean *NDVI* value ranges from 0 to 0.2; hence, an emissivity value of 0.996 was designated.

2.5.6. Determining Land Surface Temperature

The Land Surface Temperature (LST), or emissivity-corrected land surface temperature (T_s), is calculated as follows [21] using Equation (7).

$$T_s = \frac{T_b}{1 + \left[\left(\frac{\lambda BT}{p}\right)\ln \varepsilon_{\lambda}\right]} \quad (7)$$

where:

- T_s is the LST (˚C);
- BT is the at-sensor temperature (˚C);
- λ is the effective wavelength of emitted radiance (≈11.5 μm);
- ρ is the constant calculated as $\rho = hc/\sigma = 1.438 \times 10^{-2}$ mK;
- where σ is the Boltzmann constant (1.38×10^{-23} J·K^{-1});
- h is Planck's constant (6.626×10^{-34} Js);
- c is the velocity of light (2.998×10^{8} m·s^{-1}).

3. Results

3.1. Seasonal Variation in Land Surface Temperature (LST) across Parishes

3.1.1. Statistical Summary of LST across Seasons

Table 2 presents the seasonal variation in Land Surface Temperature (LST) for Baton Rouge and New Orleans parishes, summarizing the minimum, maximum, mean, and standard deviation of LST during the dry and rainy seasons. In Baton Rouge, the mean LST during the dry season is 32.53˚C, with temperatures ranging from 16.13˚C to 53.78˚C, while in the rainy season, the mean LST drops significantly to 19.26˚C, with a minimum of 0.21˚C and a maximum of 33.29˚C. Similarly, New Orleans shows a dry season mean LST of 30.90˚C, ranging from 2.07˚C to 52.86˚C, and a lower rainy season mean of 18.85˚C, with temperatures between 7.32˚C and 37.30˚C. The higher standard deviation in New Orleans during the dry season (6.59˚C) compared to Baton Rouge (3.68˚C) suggests greater spatial variability in surface temperatures. The results indicate a pronounced seasonal contrast, characterized by persistently elevated and more varied land surface temperature (LST) values throughout the dry season in both parishes, reflecting di-

minished moisture availability and heightened surface heating.

Table 2. Seasonal variation in land surface temperature (LST) across parishes in Louisiana: minimum, maximum, mean, and standard deviation of LST (˚C) during dry and rainy seasons in Baton Rouge and New Orleans.

Parish	Season	LST Min (˚C)	LST Max (˚C)	LST Mean (˚C)	SD
Baton Rouge	Dry Season	16.13	53.78	32.53	3.68
	Rainy Season	0.21	33.29	19.26	3.07
New Orleans	Dry Season	2.07	52.86	30.90	6.592
	Rainy Season	7.32	37.30	18.85	3.29

3.1.2. Seasonal Spatial Patterns of LST in New Orleans Parish

Figure 5 illustrates the spatial distribution of Land Surface Temperature (LST) in New Orleans Parish across rainy and dry seasons, supplemented with pie charts depicting the percentage of area inside each temperature classification. In the rainy season, LST values are primarily low, with 74.42% of the region between the 20.01˚C - 25˚C range and merely 0.02% surpassing 35˚C, indicating colder surface conditions attributed to increased moisture content and vegetation cover. Conversely, the dry season demonstrates much higher land surface temperature (LST)

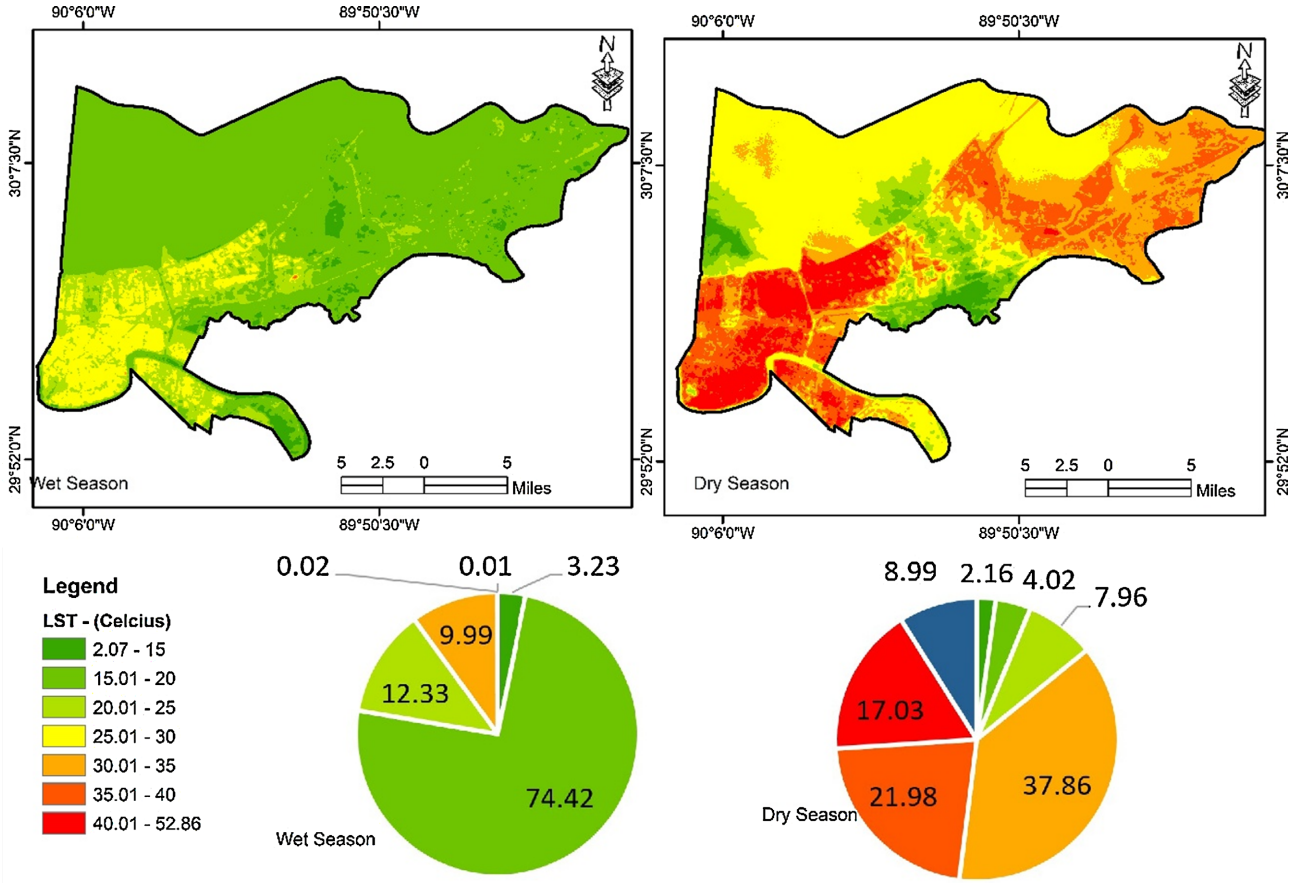

Figure 5. New Orleans parish LST from the dry and rainy season.

values, with 37.86% of the area registering temperatures between 30.01˚C and 35˚C, 21.98% between 35.01˚C and 40˚C, and 17.03% over 40˚C. The elevated temperatures, depicted by broad red and orange areas on the map, signify the effects of diminished surface moisture and heightened heat retention by impermeable surfaces. The pronounced seasonal variation highlights the impact of moisture availability and land cover on land surface temperature, with the dry season likely exacerbating urban heat island effects and thermal stress throughout the area.

3.1.3. Seasonal Spatial Patterns of LST in Baton Rouge Parish

Figure 6 depicts the spatial distribution of Land Surface Temperature (LST) in Baton Rouge Parish across rainy and dry seasons, accompanied by pie charts demonstrating the land area percentage within each temperature category. During the rainy season, the majority of the region displays reduced land surface temperature (LST) readings, with 59.76% of the area within the 20.01˚C - 25˚C range and 33.05% within the 25.01˚C - 30˚C range, suggesting predominantly cooler temperatures attributable to increased moisture content and vegetation cover. In contrast, the dry season exhibits a significant rise in surface temperatures, with 40.43% of the region registering land surface temperatures (LSTs) between 30.01˚C and 35˚C, 33.37% between 25.01˚C and 30˚C, and 23.07% beyond 35˚C. The prevalence

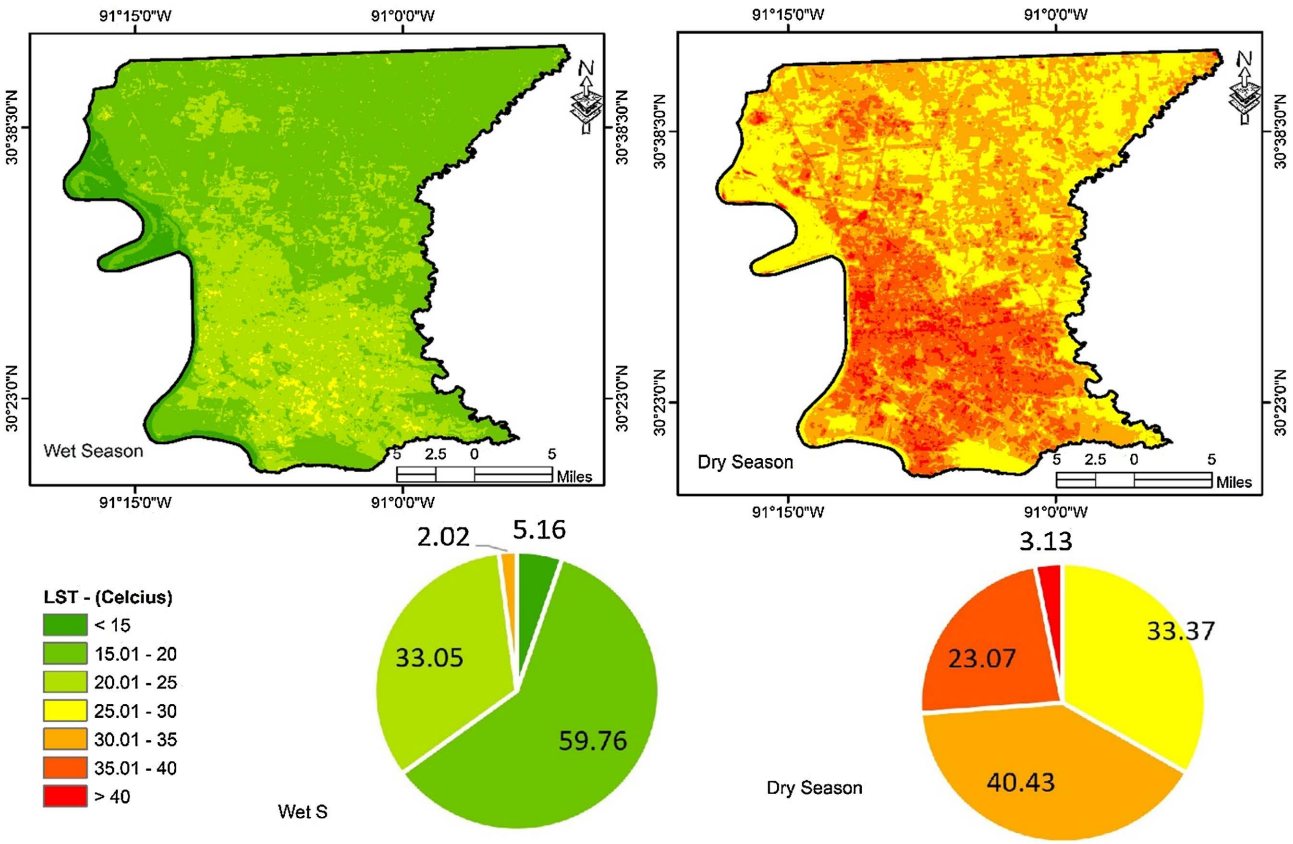

Figure 6. Baton Rouge parish LST from dry and rainy season.

of orange and red hues in the dry season map underscores the escalation of heat, possibly due to diminished moisture, heightened solar radiation, and increased exposure to impermeable surfaces. This seasonal disparity highlights the influence of hydrological and surface cover variables on regulating land surface temperature variations in Baton Rouge Parish.

4. Discussion

The analysis of seasonal variations in Land Surface Temperature (LST) across New Orleans and Baton Rouge reveals pronounced thermal differences driven by hydrological seasonality, urban morphology, and land cover characteristics. The marked contrast between dry and rainy season LSTs observed in both cities underscores the dominant role that surface moisture availability and vegetative cover play in mediating surface energy balances in humid subtropical urban settings like southeastern Louisiana.

The results clearly indicate that the dry season is associated with significantly higher LSTs in both New Orleans and Baton Rouge. In Baton Rouge, the average LST increased by approximately 13.3˚C, from 19.26˚C during the rainy season to 32.53˚C in the dry season. Similarly, New Orleans experienced a rise of 12.05˚C between seasons. This seasonal amplitude in surface temperatures can be attributed to decreased surface moisture during the dry months, leading to reduced evaporative cooling. The absence of rainfall reduces soil moisture and diminishes the transpiration of vegetation, thereby intensifying surface heating—especially over impervious surfaces such as asphalt, concrete, and rooftops.

Notably, despite both cities experiencing similar climate regimes, New Orleans exhibited a wider standard deviation in LST values during the dry season (6.59˚C) compared to Baton Rouge (3.68˚C). This finding points to greater spatial heterogeneity in surface characteristics across New Orleans, likely resulting from its complex land cover patterns—such as the juxtaposition of dense urban infrastructure, water bodies, vegetated parks, and low-lying wetland areas. These land cover variations contribute to thermal contrasts, enhancing the spatial manifestation of the urban heat island (UHI) effect in New Orleans.

The spatial analysis maps reveal that both cities exhibit significant surface warming in areas with low vegetation cover and high concentrations of impervious surfaces, especially during the dry season. Central and highly urbanized zones in both parishes displayed LSTs exceeding 40˚C, reflecting reduced evapotranspiration and increased heat storage in built environments. Conversely, areas dominated by green space or water bodies maintained lower LSTs, especially during the rainy season, illustrating the cooling benefits of vegetative and hydrological features. In Baton Rouge, more than 73% of the land area remained under 30˚C during the rainy season, as compared to only 26% during the dry season. Similarly, New Orleans saw a sharp contraction of cool surface areas in the dry season, with over 17% of its land area exceeding 40˚C, suggesting a strong heat retention capacity in its built-up core. These findings emphasize the critical role of urban greenery and

permeable surfaces in moderating surface temperatures and mitigating thermal stress in dense urban areas.

The seasonally elevated LSTs observed—particularly in the core urban areas—highlight the manifestation of the urban heat island effect, which tends to intensify during dry seasons when surface moisture is at its lowest. The UHI effect not only amplifies the thermal discomfort of residents but also has implications for energy demand, air quality, and public health, especially for vulnerable populations such as the elderly and low-income residents who may lack adequate cooling infrastructure. New Orleans' complex geography—flanked by water bodies and situated below sea level in many areas—further complicates the UHI dynamics. The city's reliance on artificial drainage and pumping systems, coupled with densely built environments, likely contributes to its relatively high thermal variability and vulnerability to heat-related impacts. Baton Rouge, though less hydrologically constrained, exhibits similar patterns in areas of commercial and residential densification. This study also focuses on intra-urban LST variations within New Orleans and Baton Rouge and does not include comparisons with surrounding rural areas. While pronounced thermal contrasts are evident across neighborhoods, the analysis does not quantify the UHI effect. The observed temperature differences primarily reflect heterogeneity in land cover, impervious surfaces, vegetation, and water bodies, underscoring the spatial complexity of the urban environment.

The use of Landsat 9 imagery and Google Earth Engine (GEE) for LST estimation provided robust, cloud-based processing of satellite-derived thermal data. However, certain limitations should be acknowledged. Firstly, Landsat's 30-meter resolution, while sufficient for general urban-scale analysis, may obscure finer-scale thermal variations found at the neighborhood or block level. Secondly, LST values may be affected by residual atmospheric noise, especially in areas with rapid transitions between land cover types, despite atmospheric correction efforts. Furthermore, this study relied on two temporal snapshots for each city—one in the dry season and one in the rainy season. While these snapshots are climatologically representative, inter-annual variations or anomalies due to short-term weather conditions or atypical rainfall events may influence surface temperature readings. Continuous or higher-temporal-resolution datasets (e.g., MODIS, ECOSTRESS) could be integrated in future work for dynamic time series analyses. A single emissivity value (0.996) was applied across the study area based on a low mean NDVI. This simplification does not account for the high spatial variability of surface materials in urban environments such as New Orleans and Baton Rouge, where impervious surfaces, vegetation, and water bodies exhibit differing emissivity values. Consequently, the absolute LST values may be subject to some uncertainty, and the spatial patterns of LST may be influenced in areas with heterogeneous land cover. Despite this, the results are considered reliable for assessing general seasonal LST trends, though caution is warranted when interpreting fine-scale variations.

The findings of this study have critical policy implications for urban planning, especially in the context of climate adaptation and heat risk reduction. Urban de-

cision-makers in Louisiana should consider integrating green infrastructure strategies, such as increasing tree canopy coverage, implementing green roofs, and expanding parklands, to lower urban LSTs. Additionally, stormwater retention systems and permeable pavements can enhance surface moisture retention, thus improving urban thermal comfort.

Future research could build on this study by comparing LST trends over multiple years to assess the long-term effects of climate change and urban expansion; integrating socio-demographic data to evaluate the intersection of LST patterns with environmental justice and vulnerability; assessing nighttime LST patterns, which are critical for understanding heat retention and recovery cycles in urban environments; and exploring machine learning approaches to predict future LST distributions under various land use and climate scenarios.

5. Conclusions

This study investigated the seasonal dynamics of land surface temperature (LST) in New Orleans and Baton Rouge using Landsat 9 satellite imagery and Google Earth Engine. The findings reveal significant seasonal variation, with substantially higher LSTs during the dry season, particularly in urbanized and impervious areas. The spatial patterns of LST underscore the strong influence of land cover, vegetation, and surface moisture on urban heat dynamics. Notably, New Orleans exhibited greater spatial variability in surface temperature, likely due to its complex urban fabric and proximity to water bodies, while Baton Rouge showed more uniform but similarly elevated temperatures in its urban core during dry months.

These results confirm the presence and seasonal intensification of the urban heat island effect in both cities, with implications for urban planning, public health, and climate resilience. As urban areas continue to expand and climate extremes become more frequent, integrating green infrastructure, enhancing surface permeability, and promoting heat-mitigation strategies will be essential for reducing thermal exposure and improving livability in Louisiana's cities. Future research should incorporate multi-year analyses and demographic overlays to explore the social dimensions of urban heat and assess how targeted interventions can equitably mitigate its impacts.

Acknowledgements

The authors would like to acknowledge the USDA National Institute of Food and Agriculture (NIFA) McIntire Stennis Forestry Research Program funded project with award number NI25MSCFRXXXG033.

Conflicts of Interest

The authors declare no conflicts of interest regarding the publication of this paper.

References

[1] Ahmed, M., Aloshan, M.A., Mohammed, W., Mesbah, E., Alsaleh, N.A. and

Elghonaimy, I. (2024) Characterizing Land Surface Temperature (LST) through Remote Sensing Data for Small-Scale Urban Development Projects in the Gulf Cooperation Council (GCC). *Sustainability*, **16**, Article 3873. https://doi.org/10.3390/su16093873

[2] Hondula, D.M., Balling, R.C., Vanos, J.K. and Georgescu, M. (2015) Rising Temperatures, Human Health, and the Role of Adaptation. *Current Climate Change Reports*, **1**, 144-154. https://doi.org/10.1007/s40641-015-0016-4

[3] Uejio, C.K., Wilhelmi, O.V., Golden, J.S., Mills, D.M., Gulino, S.P. and Samenow, J.P. (2011) Intra-Urban Societal Vulnerability to Extreme Heat: The Role of Heat Exposure and the Built Environment, Socioeconomics, and Neighborhood Stability. *Health & Place*, **17**, 498-507. https://doi.org/10.1016/j.healthplace.2010.12.005

[4] Voogt, J.A. and Oke, T.R. (2003) Thermal Remote Sensing of Urban Climates. *Remote Sensing of Environment*, **86**, 370-384. https://doi.org/10.1016/s0034-4257(03)00079-8

[5] Oke, T.R. (1982) The Energetic Basis of the Urban Heat Island. *Quarterly Journal of the Royal Meteorological Society*, **108**, 1-24. https://doi.org/10.1002/qj.49710845502

[6] Weng, Q. (2009) Thermal Infrared Remote Sensing for Urban Climate and Environmental Studies: Methods, Applications, and Trends. *ISPRS Journal of Photogrammetry and Remote Sensing*, **64**, 335-344. https://doi.org/10.1016/j.isprsjprs.2009.03.007

[7] Summers, J.K., Sanderson, R., Trahan, R., Hendricks, K., Ruffin, M., Williams, A., *et al.* (2024) Development of Community-Level Capacity of Resilience to Natural Hazards for Environmental- and Social-Justice-Challenged Communities: 1. Approach, Concepts, and Assessment of Existing Information. *Sustainability*, **16**, Article 963. https://doi.org/10.3390/su16030963

[8] Loh, P.M., Twumasi, Y.A., Ning, Z.H., Anokye, M., Frimpong, D.B., Oppong, J., *et al.* (2023) Spatiotemporal Analysis of COVID-19 Lockdown Impact on the Land Surface Temperatures of Different Land Cover Types in Louisiana. *Journal of Geographic Information System*, **15**, 458-481. https://doi.org/10.4236/jgis.2023.155023

[9] Stone Jr., B. (2012) The City and the Coming Climate: Climate Change in the Places We Live. Cambridge University Press. https://doi.org/10.1017/cbo9781139061353

[10] Weng, Q., Lu, D. and Schubring, J. (2004) Estimation of Land Surface Temperature-Vegetation Abundance Relationship for Urban Heat Island Studies. *Remote Sensing of Environment*, **89**, 467-483. https://doi.org/10.1016/j.rse.2003.11.005

[11] WeatherSpark (2025) Average Weather in Louisiana, Missouri, United States Year-Round. https://weatherspark.com/y/11482/Average-Weather-in-Louisiana-Missouri-United-States-Year-Round

[12] Ermida, S.L., Soares, P., Mantas, V., Göttsche, F. and Trigo, I.F. (2020) Google Earth Engine Open-Source Code for Land Surface Temperature Estimation from the Landsat Series. *Remote Sensing*, **12**, Article 1471. https://doi.org/10.3390/rs12091471

[13] Twumasi, Y.A., Merem, E.C., Namwamba, J.B., Mwakimi, O.S., Ayala-Silva, T., Frimpong, D.B., *et al.* (2021) Estimation of Land Surface Temperature from Landsat-8 OLI Thermal Infrared Satellite Data. a Comparative Analysis of Two Cities in Ghana. *Advances in Remote Sensing*, **10**, 131-149. https://doi.org/10.4236/ars.2021.104009

[14] Simon, O., Yamungu, N. and Lyimo, J. (2022) Simulating Land Surface Temperature Using Biophysical Variables Related to Building Density and Height in Dar Es Salaam, Tanzania. *Geocarto International*, **38**, Article ID: 2142971. https://doi.org/10.1080/10106049.2022.2142971

[15] Chander, G., Markham, B.L. and Helder, D.L. (2009) Summary of Current Radiometric Calibration Coefficients for Landsat MSS, TM, ETM+, and EO-1 ALI Sensors. *Remote Sensing of Environment*, **113**, 893-903. https://doi.org/10.1016/j.rse.2009.01.007

[16] Simon, O., Yamungu, N. and Lyimo, J. (2023) Influence of Urban Land Use Land Cover Changes on Land Surface Temperature in Dar Es Salaam Metropolitan City, Tanzania: The Use of Geospatial Approach. *Tanzania Journal of Science*, **49**, 356-368. https://doi.org/10.4314/tjs.v49i2.7

[17] Li, L., Mu, X., Jiang, H., Chianucci, F., Hu, R., Song, W., *et al.* (2023) Review of Ground and Aerial Methods for Vegetation Cover Fraction (fCover) and Related Quantities Estimation: Definitions, Advances, Challenges, and Future Perspectives. *ISPRS Journal of Photogrammetry and Remote Sensing*, **199**, 133-156. https://doi.org/10.1016/j.isprsjprs.2023.03.020

[18] Kalyan, S. and Pathak, B. (2024) Urban Sprawl Impact Assessment on the Land Surface Temperature over the Green Capital of Gujarat Using a Geospatial Approach. *Environmental Monitoring and Assessment*, **196**, Article No. 866. https://doi.org/10.1007/s10661-024-13038-7

[19] Zheng, X., Guo, Y., Zhou, Z. and Wang, T. (2024) Improvements in Land Surface Temperature and Emissivity Retrieval from Landsat-9 Thermal Infrared Data. *Remote Sensing of Environment*, **315**, Article ID: 114471. https://doi.org/10.1016/j.rse.2024.114471

[20] Hu, L., Sun, Y., Collins, G. and Fu, P. (2020) Improved Estimates of Monthly Land Surface Temperature from MODIS Using a Diurnal Temperature Cycle (DTC) Model. *ISPRS Journal of Photogrammetry and Remote Sensing*, **168**, 131-140. https://doi.org/10.1016/j.isprsjprs.2020.08.007

[21] Stathopoulou, M. and Cartalis, C. (2007) Daytime Urban Heat Islands from Landsat ETM+ and Corine Land Cover Data: An Application to Major Cities in Greece. *Solar Energy*, **81**, 358-368. https://doi.org/10.1016/j.solener.2006.06.014